Journal of Materials Chemistry B

ROYAL SOCIETY OF CHEMISTRY

PAPER

View Article Online
View Journal | View Issue

Cite this: J. Mater. Chem. B, 2022, 10, 47

Functionalization of filled radioactive multi-walled carbon nanocapsules by arylation reaction for *in vivo* delivery of radio-therapy†

Agnieszka Gajewska,‡[a] Julie T.-W. Wang,‡[b] Rebecca Klippstein,[b] Markus Martincic,[c] Elzbieta Pach,[d] Robert Feldman,[e] Jean-Claude Saccavini,[e] Gerard Tobias,[c] Belén Ballesteros,[d] Khuloud T. Al-Jamal *[b] and Tatiana Da Ros *[a]

Functionalized multi-walled carbon nanotubes (MWCNTs) containing radioactive salts are proposed as a potential system for radioactivity delivery. MWCNTs are loaded with isotopically enriched 152-samarium chloride ($^{152}SmCl_3$), the ends of the MWCNTs are sealed by high temperature treatment, and the encapsulated ^{152}Sm is neutron activated to radioactive ^{153}Sm. The external walls of the radioactive nanocapsules are functionalized through arylation reaction, to introduce hydrophilic chains and increase the water dispersibility of CNTs. The organ biodistribution profiles of the nanocapsules up to 24 h are assessed in naïve mice and different tumor models *in vivo*. By quantitative γ-counting, $^{153}SmCl_3$@MWCNTs-NH_2 exhibite high accumulation in organs without leakage of the internal radioactive material to the bloodstream. In the treated mice, highest uptake is detected in the lung followed by the liver and spleen. Presence of tumors in brain or lung does not increase percentage accumulation of $^{153}SmCl_3$@MWCNTs-NH_2 in the respective organs, suggesting the absence of the enhanced permeation and retention effect. This study presents a chemical functionalization protocol that is rapid (∼one hour) and can be applied to filled radioactive multi-walled carbon nanocapsules to improve their water dispersibility for systemic administration for their use in targeted radiotherapy.

Received 7th October 2021,
Accepted 19th November 2021

DOI: 10.1039/d1tb02195h

rsc.li/materials-b

Introduction

Carbon nanotubes (CNTs) can be categorized as single- and multi-walled carbon nanotubes (SWCNTs and MWCNTs, respectively).[1] SWCNTs are characterized as thinner and more reactive on the surface whereas MWCNTs, in contrast to SWCNTs, have remarkably better dispersibility, resistance for processing and higher capacity for internal filling. Generally speaking, both types of CNTs have very promising characteristics, which can be useful for biological applications.[2] One very important advantage of CNTs is the ability to cross biological barriers with a small cytotoxic effect.[3] This makes them an excellent host material for several therapeutic agents where different parameters can be modified to obtain the best biological effect.[4]

The carbon nanotubes can be subjected to external functionalization by attaching various moieties on the outside of the tubes, but they can also be modified by filling the inner cavity with various compounds, with an endohedral approach. The resulting filled CNTs are described as X@CNTs where X indicates the content of the tube.

In the last decade, rational design and assembly of novel tumor-targeting radiopharmaceuticals has risen under the concept of cancer treatment and diagnosis. In a perfect situation, radiopharmaceuticals should target tumor tissues with small overall loss of radionuclides in the body and supply highest dosage of radiation. With this regard, among other vehicles as calcium carbonate microstructures,[5] CNTs have been proposed as model radioactivity carriers to deliver the specific irradiation in cancer-affected tissues and improve the outcome of diagnosis and treatment. A limited number of examples of radioactive CNTs have been reported in the literature so far. For the

[a] INSTM, Trieste Unit & Department of Chemical and Pharmaceutical Sciences, University of Trieste, Via Licio Giorgieri 1, 34127 Trieste, Italy. E-mail: daros@units.it
[b] School of Cancer and Pharmaceutical Sciences, Faculty of Life Sciences & Medicine, King's College London, London SE1 9NH, UK. E-mail: khuloud.al-jamal@kcl.ac.uk
[c] Institut de Ciència de Materials de Barcelona (ICMAB-CSIC), Campus UAB, 08193 Bellaterra, Barcelona, Spain
[d] Catalan Institute of Nanoscience and Nanotechnology (ICN2), CSIC and the Barcelona Institute of Science and Technology, Campus UAB, 08193 Bellaterra, Barcelona, Spain
[e] Cis Bio International Ion Beam Applications SA (IBA), 91400 Saclay, France

† Electronic supplementary information (ESI) available: Additional figures and synthesis details as described in the text. See DOI: 10.1039/d1tb02195h

‡ These authors equally contributed.

first time the activity of such system in a biological media was reported on SWCNTs filled with NaI. Hong *et al.* presented SWCNTs filled with $Na^{125}I$ (Auger and γ-emitter), functionalized and glycosylated for *in vitro* and *in vivo* studies.[6] The material had a specific tissue accumulation in lungs due the physical properties of the SWCNTs in a physiological context.[7] Remarkably, leakage of the radionuclide was not observed in comparison to nanotubes where radioisotopes were externally bounded (^{86}Y, ^{111}In, ^{14}C, ^{64}Cu or ^{99m}Tc).[8] Pascu *et al.* have given versatility to the encapsulation approach by sealing ^{64}Cu inside the cavities of SWCNTs.[9] The containment of radionuclides was achieved by using fullerenes as corks, and the external walls were non-covalently wrapped with β-D-glucan.

Among several isotopes used in radiotherapy, Spinato *et al.* tested two radionuclide analogues ($SmCl_3$ and $LuCl_3$) encapsulated in SWCNTs for targeted anticancer therapy. They reported the functionalization of metal halides-filled and sealed nanotubes by nitrene cycloaddition. Conjugation with a monoclonal antibody (Cetuximab) showed improved cancer cell targeting *in vitro*.[10] For both filled SWCNTs, it was observed that the functionalization allowed the active endocytosis and "nanoneedle" mechanism, a passive trans-location into the cytoplasm, previously reported.[11] No significant reduction in viability was observed *in vitro*. This finding is very promising for the application of radioactive carbon nanotubes-based materials because the entrapment of the isotope could prevent its leakage in an uncontrolled manner under complex environment *in vivo*.

These observations prompted our current work focusing on the application of functionalized MWCNTs as delivery systems for therapeutic and diagnostic radioisotopes. Nanocapsules composed of MWCNTs are likely to offer a higher loading capacity for radioactive isotopes, better resistance for processing and lower uncontrolled release of the radioisotopes in the organism compared to SWCNTs. Functionalization by covalent decoration of their external walls is necessary to provide better dispersibility and biocompatibility and to facilitate subsequent modification with targeting ligands. The choice of the functionalization methodology for such purposes should be carefully selected in such a way that functionalization reaction is highly efficient while keeping its duration minimal, especially important for short-lived radionuclides. The reaction needs to be mild not to damage the walls integrity which may cause premature release of the previously sealed metals. Oxidation-based reaction approaches are naturally excluded. In this study, we propose a modified Tour reaction functionalization approach with triazine units being introduced to the walls of $SmCl_3$ filled-MWCNTs. It was possible to shorten the reaction time down to 1 h, without significantly decreasing the functionalization degree.[12] The functionalized MWCNTs were fully characterized prior to studying their bio-interactions with cells and organ biodistribution in different types of tumor-bearing mice. Cytotoxicity of non-functionalized and functionalized nanocapsules at different concentrations was assessed in murine B16F10 melanoma and J774 macrophages. Functionalization was performed on radioactive $SmCl_3$ filled-MWCNTs, irradiated by neutron activation.[13] The organ biodistribution profiles were established and tumor uptake were examined up to 24 h in naïve mice and in tumor-bearing mice (GL261 glioma model, B16F10 melanoma implanted subcutaneously and B16F10 melanoma experimental lung metastasis model) by quantitative γ-counting, following intravenous injection.

Results

Filling of MWCNTs with samarium

In the first step, MWCNTs were treated by oxidative purification followed by steam treatment to shorten the nanotubes, remove metal and amorphous carbon impurities. TGA of purified MWCNTs were performed under flowing air for quantification of the inorganic impurities in the samples deriving from the synthesis of the nanotubes. The amount of inorganic solid residue after the TGA analysis turned out to be 1.2 wt%. Since iron is used as catalyst for the growth of MWCNTs, the residue after the oxidative analysis will consist of Fe_2O_3, assuming that no other impurities are present. Therefore, a 1.2 wt% residue corresponds to a 0.8 wt% of iron catalyst in the sample (ESI,† Fig. S1a). MWCNTs underwent endohedral functionalization with samarium chloride ($SmCl_3$) by molten phase high temperature filling. The filled, closed-ended tubes were then purified with acidic water and filtered to remove the non-encapsulated $SmCl_3$. After this step, from TGA results it was possible to calculate the filling yield using a previously reported formula[14] and a filling yield of 17 wt% was obtained (Fig. S1b, ESI†). The encapsulation of the metal halides in the internal cavities of MWCNTs was confirmed by electron microscopy imaging. By HAADF STEM imaging, direct visualization of the encapsulated material was achieved and a high degree of filling can be observed (Fig. 1a). The filling appears with a bright intensity whereas the carbon nanotubes are seen in a pale grey contrast.[15] The evidence of the confinement of the materials inside MWCNTs was also provided by high resolution TEM imaging (Fig. 1b) where the encapsulated $SmCl_3$ was seen to adopt both nanowire and single-layered nanotube structures, as has been previously reported.[16] Further confirmation of the filling was achieved with energy dispersive X-ray spectroscopy (EDX) coupled to the transmission electron microscope. EDX analyses (Fig. 1c) revealed the presence of $SmCl_3$ and the absence of impurities (note that the Cu peak arises from the TEM support grid).

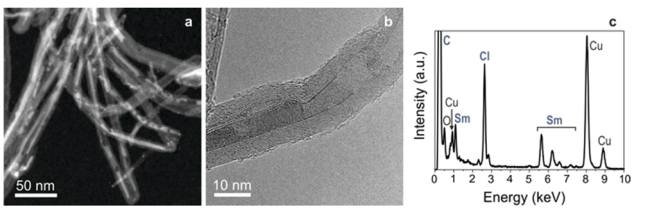

Fig. 1 (a) HAADF-STEM image of $SmCl_3$@MWCNTs; (b) HRTEM image $SmCl_3$@MWCNTs; (c) $SmCl_3$@MWCNTs EDX spectrum showing the presence of samarium and chlorine atoms.

Functionalization of samarium-filled MWCNTs

The covalent functionalization of filled MWCNTs was carried out *via* aryl diazonium chemistry.[17] The reaction has been reported first by Tour, and later performed by many other authors as a highly reactive pathway for the sidewall decoration of SWCNTs and also MWCNTs[12,18] under mild conditions using aniline derivatives. It is postulated that the electron from the CNTs is transferred onto diazonium salt, and then after elimination of N_2 a reactive aryl radical is formed.[19] Usually, this reaction is performed under heating for long periods but we previously reported an optimized approach with short reaction time (1 h).[12] Working with radioactive materials requires to be as fast as possible to minimize the radioactivity decay during the reaction, especially if in presence of short living species. Another crucial aspect of the functionalization to be taken into account is the necessity to minimize the radioactive contaminated waste. The functionalization process was first optimized using cold materials using minimum quantities of solvents, and then applied to the hot $^{153}SmCl_3$@MWCNTs. The synthesis is described in Scheme 1. In order to enhance the water-dispersibility of filled tubes and to offer functional side chains, an aniline bearing a triazine unit was modified with two aminoethylene glycol chains (Scheme 1). With this approach, it was possible to introduce two solubilizing appendages per aryl unit. The functionalization was initially performed on cold $SmCl_3$@MWCNTs, and later with $^{152}SmCl_3$@MWCNTs, using a 25-fold mass excess of aniline derivative. The mixture was stirred at 80 °C for 1 h. To functionalize MWCNTs containing γ-emitter ^{153}Sm, a quantity of cold isotopically enriched material was added to the radioactive compound to have a manageable quantity of materials to perform the reaction and the same procedure of functionalization and cleavage was applied on the hot mixture (Scheme 1).

Afterwards, the solution was filtered and washed by cycles of ultrasonication and filtration using different solvents to guarantee a clean sample. The phthalimide protecting group was cleaved from $SmCl_3$@MWCNTs-Pht by hydrazine in ethanol.

Characterization of functionalized, filled multi-walled carbon nanotubes

Thermogravimetric analysis (TGA). The characterization was carried out on the cold sample by TGA in air (Fig. 2a) and in nitrogen gas flow (Fig. 2b). The small reduction in the percentage of collected solid residue at 650 °C in air is consistent with the increase in the organic portion of the sample itself, due to the presence of external functionalities. The absence of huge reduction in mass confirmed that the filling content was retained after the organic functionalization.

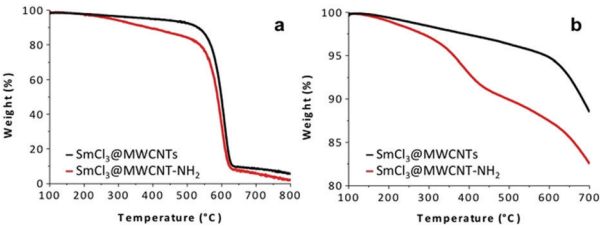

Fig. 2 TGA profiles of $SmCl_3$@MWCNTs (–) and functionalized $SmCl_3$@MWCNTs-NH_2 (–), (a) in air; (b) in N_2 atmosphere.

The degradation process under inert atmosphere was monitored to determine the degree of functionalization obtained using derivative 1 (see Scheme 1), in the temperature ranging between 100 and 700 °C (Fig. 2b). The weight loss observed between 250 and 550 °C was attributed to the degradation of the organic decoration and corresponds to a loading of 90 μmol (triazine derivative) g^{-1}. The free amine content on functionalized $SmCl_3$@MWCNTs-NH_2 was determined by colorimetric Kaiser test (60 μmol g^{-1}). In both cases (TGA and Kaiser test), the content of encapsulated salt was taken into account to calculate the functionalization values.

Transmission electron microscopy. The sample was subjected to microscopic characterization. Images of the functionalized filled nanotubes reveal their high degree of individualization. Additionally, no leakage of the filled metal halide after functionalization or ultrasonic treatment was detected, and it preserved the structure as nanowires and nanotubes that was present before the functionalization step (Fig. 3a), proving that the internal part

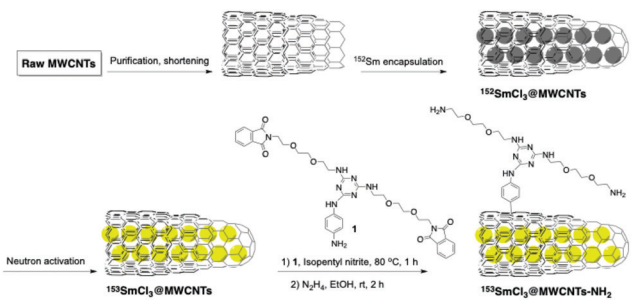

Scheme 1 Synthesis of $^{153}SmCl_3$@MWCNTs-NH_2.

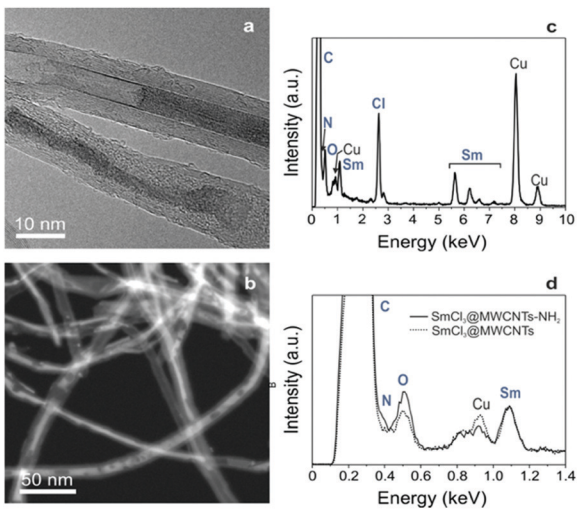

Fig. 3 (a) HRTEM image of $SmCl_3$@MWCNTs-NH_2; (b) HAADF-STEM image of $SmCl_3$@MWCNTs-NH_2; (c) EDX spectrum of $SmCl_3$@MWCNTs-NH_2, (d) EDX spectra of $SmCl_3$@MWCNTs-NH_2 (solid line) and $SmCl_3$@MWCNTs (dotted line) in the 0–1.4 keV range.

of the $SmCl_3$@MWCNTs-NH_2 was undisturbed throughout the whole synthetic procedure. Expectedly, HAADF-STEM images confirmed the high degree of filling (Fig. 3b), and EDX analyses revealed an increase in the amount of oxygen and nitrogen after chemical functionalization (Fig. 3c and d).

Cytotoxicity of $^{152}SmCl_3$@MWCNTs in B16F10-Luc and J774 cells

To assess how filled non-radioactive MWCNTs (both non-functionalized and functionalized) can affect cell survival, cytotoxicity tests were performed using melanoma B16F10-Luc and macrophages J774 cells. Both $^{152}SmCl_3$@MWCNTs and $^{152}SmCl_3$@MWCNTs-NH_2 were dispersed in 1% Pluronic F-127. To better compare the effect of chemical functionalization on cell viability, functionalized $^{152}SmCl_3$@MWCNTs-NH_2 dispersed in water were also prepared for comparison. Cells were incubated with 10, 50 and 100 μg mL^{-1} of CNTs for 72 h. Cells exposed to 10% DMSO and the surfactant alone were used as controls.

The cytotoxicity was determined by the modified LDH assay (Fig. 4 and Fig. S2, ESI†).[20] Cells incubated in media containing the same amount of Pluronic F-127 did not show obvious reduction in cell viability (Fig. 4, light grey bars). In the case of B16F10-Luc cells (Fig. 4a), the 72 h-exposure of both CNT types did not cause significant cytotoxicity in most of the tested conditions (>80% cell viability), except treatments of $^{152}SmCl_3$@MWCNTs-NH_2 at higher concentrations (*i.e.* 50 and 100 μg mL^{-1}). In the case of J774 cells (Fig. 4b), a dose-dependent reduction in cell viability was found with significant toxicity observed at 100 μg mL^{-1} ($p < 0.001$). In B16F10-Luc cells, no significant difference was observed between CNTs dispersed in water and in Pluronic F-127. In contrast, as observed in J774 cells, $^{152}SmCl_3$@MWCNTs-NH_2 dispersed in water were less toxic than those dispersed in Pluronic F-127 at 100 μg mL^{-1} ($p < 0.001$) (Fig. 4b).

Neutron irradiation

Part of the so-obtained batch of filled $^{153}SmCl_3$@MWCNT was activated as described above. The specific radioactivity (SRA) values of the sample were measured as 15.97 GBq per mg of $^{153}SmCl_3$@MWCNTs after neutron irradiation for 78 h.

Blood clearance, excretion and organ biodistribution profiles of $^{153}SmCl_3$@MWCNTs-NH_2 in naïve mice

The blood clearance profile of $^{153}SmCl_3$@MWCNTs after intravenous injection is presented in Fig. 5a. $^{153}SmCl_3$@MWCNTs displayed fast clearance from the circulation within the first 1 h after injection. To study the excretion profile of the $^{153}SmCl_3$@MWCNTs-NH_2, animals were housed in metabolic cages (one mouse per cage) and the urine and feces were collected at 24 h post-administration followed by γ-counting (Fig. 5b). It was found that negligible amounts (<0.02% of total injected dose) were eliminated into urine and feces.

The biodistribution of $^{153}SmCl_3$@MWCNTs-NH_2 in major organs in mice was assessed at 1, 4 and 24 h after intravenous injection. As shown in Fig. 5c, mice treated with $^{153}SmCl_3$@MWCNTs-NH_2 showed the highest uptake in lung (88.8 ± 23.5% ID g^{-1}) followed by liver (7.4 ± 0.8% ID g^{-1}) and spleen

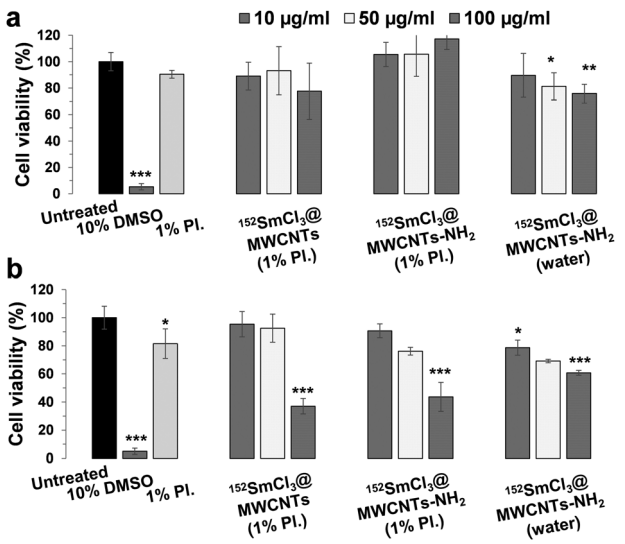

Fig. 4 Cytotoxicity of the non-radioactive $^{152}SmCl_3$@MWCNTs and $^{152}SmCl_3$@MWCNTs-NH_2 on two cell lines B16F10-Luc and J774 after incubation of 72 h. (a) B16F10 cells and (b) J774 cells were incubated with $^{152}SmCl_3$@MWCNTs in 1% Pluronic F-127 (1% Pl.) and $^{152}SmCl_3$@MWCNTs-NH_2 in 1% Pluronic F-127 and water at 10, 50 and 100 μg mL^{-1} for 72 h. Cytotoxicity was examined by modified LDH assay. Data are presented as mean ± standard deviation (n = 3–4). Statistical analysis was performed using one way ANOVA with respect to untreated group. *$p < 0.05$, **$p < 0.01$, ***$p < 0.001$.

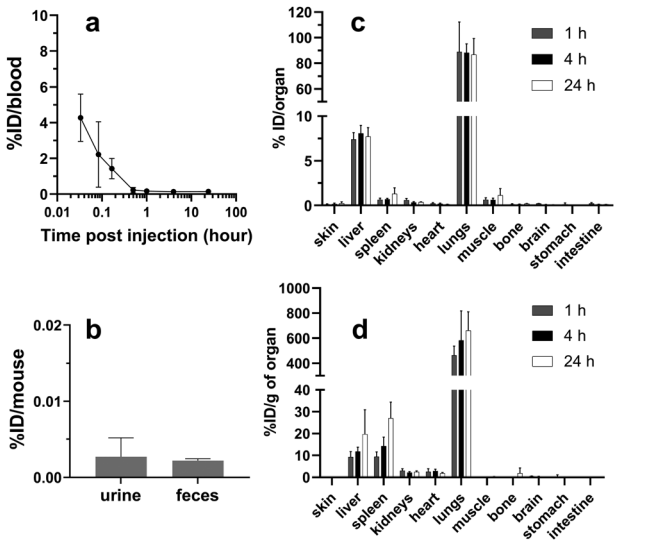

Fig. 5 *In vivo* biodistribution of $^{153}SmCl_3$@MWCNTs-NH_2 in naïve mice up to 24 h following intravenous injection. Naïve C57BL/6 mice were injected with 200 μg of $^{153}SmCl_3$@MWCNTs-NH_2 containing ~1.5 MBq. For excretion profiles, mice were housed individually in metabolic cages with the urine and feces collected for 24 h after injection. The radioactivity of blood and major organs sampled at specified time points, and urine/feces collected at 24 h post-injection, were measured by γ-counting. The results are expressed as % ID in blood (a), % ID in urine/feces per mouse (b) and % ID/organ and g of organ (c and d), and presented as mean ± S.D. (n = 3).

($0.9 \pm 0.6\%$ ID g^{-1}) at 1 h post-injection. No significant change in the uptake in lung and liver was observed over time.

Organ biodistribution and tumor uptake of $^{153}SmCl_3$@MWCNTs-NH_2 in tumor-bearing mice

The organ biodistribution profiles of $^{153}SmCl_3$@MWCNTs-NH_2 in different tumor models at 1 and 24 h post-injection are shown in Fig. 6 and Fig. S3 (ESI†). No obvious alterations of the biodistribution patterns were observed between naïve and tumor-bearing mice, with highest accumulation found in lung, followed by liver and spleen (Fig. 6a). The comparison of the uptake in cancerous tissues (glioma, s.c. melanoma and experimental lung metastatic melanoma) and the corresponding tissues in naïve mice (*i.e.* brain and lung) are shown in Fig. 6b. No significant differences were observed in glioma brain ($\sim$0.8% ID g^{-1} tissue) and lung metastatic melanoma ($\sim$400% ID g^{-1} tissue) compared to healthy brain and lung, respectively (data from the above biodistribution study in naïve mice). Doses found in s.c. melanoma tumors at 1 h were in the range of $\sim$0.4% ID g^{-1} tissue. The uptake in organs decreased from 1 h to 24 h in glioma brains and s.c. tumors but not in lungs. Retention of $^{153}SmCl_3$@MWCNTs-NH_2 was observed in naïve lungs or cancerous lungs (Fig. 6b, bottom graph). It is worth noting that these measurements were done on perfused animals so values in the organs are unlikely to be related to organ contamination with circulating blood.

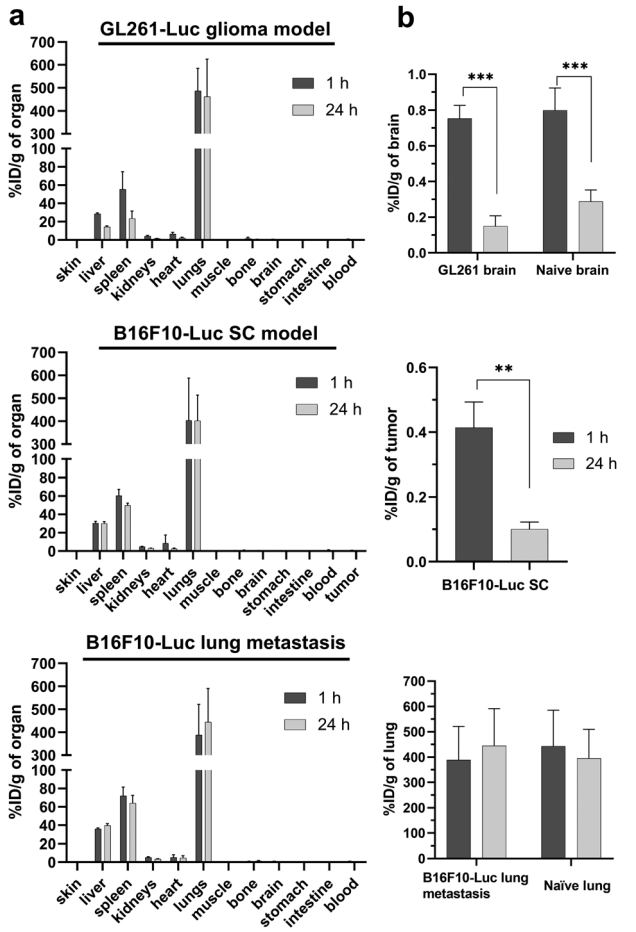

Fig. 6 *In vivo* biodistribution of $^{153}SmCl_3$@MWCNTs-NH_2 in tumour-bearing mice at 1 h and 24 h post-injection. (a) Organ biodistribution profiles in intra-cranial GL261-Luc glioma model (top), subcutaneous B16F10-Luc (B16F10-Luc SC, middle) and B16F10-Luc lung metastasis model (bottom). (b) Uptake in tumours and tumour-containing tissues. Naïve C57BL/6 mice were injected with 200 μg of $^{153}SmCl_3$@MWCNTs-NH_2 containing $\sim$1.5 MBq. The radioactivity of blood and major organs sampled at 1 h and 24 h post-injection was measured by γ-counting. The results expressed as % ID g^{-1} of organ and presented as mean ± S.D. (n = 3). The data of tumour accumulation in (b) were extracted from (a) and the data of naïve tissues for comparison were extracted from Fig. 5. Statistical analysis was performed using one way ANOVA with respect to untreated group. $^{**}p < 0.01$, $^{***}p < 0.001$.

Discussion

In the first report on carbon nanocapsules (closed-ended filled carbon nanotubes) for *in vivo* radioemitter, SWCNTs were filled with $Na^{125}I$, then covalently functionalized by 1,3-dipolar cycloaddition and glycosylated.[6] The study highlighted the specific organ (lung) accumulation and absence of isotope leakage from the $GlcNAc^{D}$-$Na^{125}I$@SWCNTs which allowed for non-invasive imaging as well as precise localization of a highly concentrated ''radiodose''. More recently, the *in vivo* fate of $Na^{125}I$@SWCNTs externally functionalized with other glycans has also been explored.[7] However, the functionalization strategy employed in these previous studies required a 96 h reflux of the reaction mixture. This was possible because the employed radionuclide (^{125}I) had a half-life of 59.5 days. However, the majority of clinically employed radionuclides have much shorter half-lives and therefore the chemical functionalization method and sub-sequent purification steps are considered to be lengthy for this application, where shortening step time is very important to minimize chance of isotope decay. Towards this end, non-covalent functionalization with β-D-glucan has been employed for ^{64}Cu@SWCNTs.[9] Herein we have developed a fast, scalable and efficient covalent strategy for the functionalization of 'hot' nanocapsules in which the functionalization requires 1 h followed by easy and fast work up. The deprotection of Fmoc groups takes place in 2 h, with a total of maximum 4 h for the complete functionalization and collection of the desired products.

When it comes to filling strategies, in early studies the filling method employed relied on the use of 'hot' (radioactive) material. Taking into account the time constraints imposed by the use of short-lived radionuclides, we have recently developed a modified method by initially filling the inner cavity of the tubes with cold material, ^{152}Sm enriched $SmCl_3$, that can then be neutron irradiated to yield $^{153}SmCl_3$.[13] Additionally, to improve the filling yield further, MWCNTs were employed for radioemitter delivery. MWCNTs have a larger inner diameter thus a higher capacity for internal loading, and a better chance for delivery of higher dose of isotope compared to SWCNTs.[3,21] Furthermore, MWCNTs present a higher resistance to structural damage by neutron irradiation than their single-walled

counter parts.[13] The specific activity of the resulting $^{153}SmCl_3$@MWCNTs is much higher than the ones previously reported for ^{125}I@SWCNTs and ^{64}Cu@SWCNTs allowing the injection of a smaller dose of tubes with higher radioactivity.

Combined with the previous efforts to improve the specific radioactivity of the filled nanocapsules, this work offers the added advantage of developing a chemical functionalization method that is sufficiently quick to allow functionalization of nanocapsules with short half-lived emitters so the radionuclides retain most of their radioactivity. In fact, starting from the well-known Tour procedure, it was possible to optimize the reaction shortening the time down to 1 h, without significantly decreasing the functionalization degree. The first attempt in this direction, to enhance the performance, was recently reported by us and used as guideline for this work,[12] while the usually reported procedures for Tour reaction are overnight[17a,c] and other successful methodologies can take overnight as well,[22] or even days.[23] The latter are obviously not applicable in the present case, taking into account the necessity to exploit as much as possible the ^{153}Sm radioactivity, the half-life of which is 46.3 h, as already mentioned. Using the optimized Tour reaction, it was possible to chemically functionalize CNT walls with a linker that decreases aggregation thanks to the free amine functional groups, which are also available for further binding with targeting molecules.

The cytotoxicity experiments were performed using J744 cells, a phagocytic cell line and B16F10-Luc cells, one of the cell lines used as tumor models *in vivo*. Cells were treated with non-functionalized and functionalized cold filled nanocapsules, dispersed in 1% Pluronic solution or water to evaluate the effect of CNT functionalization and presence of surfactant on cell viability.

To properly suspend the non-functionalized nanocapsules and to use them in the cytotoxicity test and in the *in vivo* analyses, the presence of Pluronic was necessary. Taking this into account, the $SmCl_3$@MWCNTs-NH_2 suspensions were prepared both without and with the surfactant, to be able to properly correlate the results to the carbon nanomaterials avoiding any external interference, and to be able at the same time to correlate the *in vivo* behavior of the non-functionalized and the functionalized nanocapsules in the same conditions.

No obvious cytotoxicity was induced when cells were treated with all preparations at the lower concentration (10 μg mL^{-1}) up to 72 h. At higher concentrations, B16F10-Luc cells were less affected than macrophages by these treatments. This could be due to the phagocytic nature of J774 cells that more materials were taken up by cells than B16F10-Luc cells.[24]

In our study, we investigated the *in vivo* biodistribution profiles of $^{153}SmCl_3$@MWCNTs-NH_2 (Fig. 5 and 6, and Fig. S3, ESI†), functionalized with alternative aryl diazonium chemistry, to provide new platform for further targeting purposes. By quantitative gamma counting, the results indicated high affinity to lung for up to 24 h in naïve mice and diseased tumor models. Moreover, small amount of $^{153}SmCl_3$@MWCNTs was detected in blood after injection (*e.g.* ~4% ID measured at 2 min post-injection) with a complete clearance from blood after 1 h. The absence of isotope in blood, urine and feces after 24 h suggests no-leakage from the tubes and high affinity to the organs.

It is also noted that $^{153}SmCl_3$@MWCNTs-NH_2 seemed to be able to reach brain, at early time post-injection (*i.e.* ~0.75% ID g^{-1} of brain detected at 1 h) (Fig. 6a). The brain uptake property of functionalized MWCNTs undergone different chemical approaches compared to the current study has been reported previously.[25,26] The feature of initial brain uptake of the studied $^{153}SmCl_3$@MWCNTs-NH_2 after injection provides another possible future application of delivering radioactivity to treat brain tumors.

It has been reported that $SmCl_3$-filled SWCNTs, conjugated with a targeting ligand, were able to improve the internalization into cancer cells *in vitro*.[10] Future work will focus on developing targeted $^{153}SmCl_3$@MWCNTs-NH_2 to achieve active targeting toward cancer.

Experimental

Materials

Solvents used for synthesis were analytical grade and were purchased from Aldrich, Acros, and Alfa Aesar. When anhydrous conditions were required, high quality commercial solvents were used (THF, DCM, toluene, DMF). Deuterated solvents were from Aldrich and Cambridge Isotope Laboratories. Water was purified using a Millipore filter system MilliQ®. Elicarb® MWCNTs were provided by Thomas Swan & Co. Ltd. MWCNTs were produced by the catalytic chemical vapor deposition process and supplied as a dry powder. Sm_2O_3 (with natural isotopic composition) was purchased from Sigma-Aldrich and enriched $^{152}Sm_2O_3$ from Eurisotop. Nanotubes filtrations were performed using Millipore JHWP filters, pore size 0.45 μm. Kaiser test kit was purchased from Sigma Aldrich. RPMI-1640 media, penicillin/streptomycin, Trypsin/EDTA, and phosphate buffered saline (PBS) were obtained from Gibco, Thermo Fisher Scientific (UK). D-Luciferin potassium salt was from PerkinElmer (UK). Murine melanoma cells B16F10-Luc and murine glioma cells GL261-Luc were purchased from PerkinElmer (UK). Mouse macrophage cells J774 were purchased from ATCC (ATCC® TIB-67™). Fetal bovine serum (FBS) was obtained from First Link UK Ltd. CytoTox 96® Non-Radioactive Cytotoxicity Assay kit was purchased from Promega UK.

Preparation of filled MWCNTs ($SmCl_3$@MWCNTs and $^{152}SmCl_3$@MWCNTs)

As-received MWCNTs were treated with a mixture of nitric/sulfuric acids followed by 1 h steam treatment following a previously described protocol.[27] The resulting short open-ended and purified MWCNTs were filled with samarium(III) chloride ($SmCl_3$) by molten phase capillary filling. When using high temperature filling, the ends of the CNTs spontaneously close on cooling thus leading to close-ended CNTs, that we refer to as carbon nanocapsules.[13,16] Anhydrous $SmCl_3$ was synthesized starting from Sm_2O_3.[28] MWCNTs were then mixed with

the freshly prepared $SmCl_3$ (w/w 1 : 10) and grinded in an agate mortar and pestle in an argon-filled glovebox. The mixture was sealed under vacuum inside a silica tube. The sample was then annealed in a horizontal furnace at 1200 °C for 12 h, well above the melting point of $SmCl_3$, to allow the formation of carbon nanocapsules. The resulting sample contained filled closed-ended nanotubes and external crystals of $SmCl_3$. The non-encapsulated material was removed by washing the sample in hot acidic water (*ca.* 200 mL of water containing 3–5 mL of concentrated HCl). MWCNTs were first soaked in the acidic water and the sample was collected after filtration over a polycarbonate membrane (0.2 μm pore size). This was followed by washing the sample in fresh acidic water with constant stirring, at 80 °C for 24 h, repeated three times, with the filtration step in between washings and change of the acidic water. After completing the washing with acidic water, a final step was added, using the same conditions (80 °C, 24 h of stirring), with 200 mL of water without acid. The same protocol was employed for the encapsulation of 152-samarium(III) chloride ($^{152}SmCl_3$), using isotopically enriched $^{152}Sm_2O_3$ as starting material. The non-irradiated filled MWCNTs are referred to as $^{152}SmCl_3$@MWCNTs.

Neutron activation of $^{152}SmCl_3$@ MWCNTs

To maximize the activation of the materials, the MWCNTs were filled with ^{152}Sm enriched samarium chloride and then activated in a neutron flux. The neutron activation was performed at the atomic reactor in Saclay (France). In brief, a silica ampoule containing 15 mg of $^{152}SmCl_3$@MWCNTs was irradiated at a neutron flux of 1×10^4 n cm^{-2} s^{-1} for 78 h. The ampoule was allowed to cool down and the radioactivity was measured using a dose calibrator (VDC 404, Veenstra Instruments, the Netherlands). The ampoule was then shattered, and the now radioactive filled MWCNT ($^{153}SmCl_3$@MWCNTs) powders were suspended in DMF. The so-obtained ^{153}Sm decays by emission of weak γ-rays and β-particles, with a half-life of 46.3 h.

Functionalization of $SmCl_3$@MWCNTs and $^{152}SmCl_3$@ MWCNTs

Due to the high cost of the isotopically enriched material, the functionalization of filled MWCNTs was initially optimized using $SmCl_3$ with natural isotopic composition. $SmCl_3$@MWCNTs (30 mg) were dispersed in 15 mL of DMF by sonication for 5 min. Then compound 1 (see Scheme 1 and Scheme S1, ESI,† 750 mg, 0.88 mmol) was added in 15 mL of DMF, dispersed for another 5 min and cooled to 0 °C (Scheme 1). Isopentyl nitrite (705 μL, 5.1 mmol) was added and reaction mixture was heated up to 80 °C and stirred for 1 h. Then, the cooled mixture was recovered by filtration, washed with DMF until the eluted solvent was colorless, re-dispersed in DMF (×2), filtered, washed with water, MeOH, EtOAc, Et_2O and dried under vacuum.

For the cleavage of amine protecting groups, 30 mg of the CNTs were dispersed in EtOH (27 mL) by sonication for 10 min, and afterwards treated with hydrazine hydrate (3 mL). The dispersion was stirred at r.t. for 2 h, and then diluted with EtOH (15 mL) and filtered. After filtration, MWCNTs were re-precipitated in EtOH, filtered, washed with 0.1 M HCl solution, water, MeOH, diethyl ether finally dried under vacuum to afford functionalized $SmCl_3$@MWCNTs bearing free amino groups (SmC_3@MWCNTs-NH_2). The same protocol was performed starting with $^{152}SmCl_3$@ MWCNTs, and the resulting functionalized sample is referred to as $^{152}SmCl_3$@MWCNTs-NH_2.

Functionalization of $^{153}SmCl_3$@ MWCNTs

The functionalization of the neutron activated $^{153}SmCl_3$@ MWCNTs was performed in a radiolab at King's College London. The specific activity obtained prior to chemical functionalization was 2.11 GBq mg^{-1} of CNTs. In this experiment, 6 mg of cold $^{152}SmCl_3$@MWCNTs (1 mg mL^{-1}) were mixed with 45 μg of radioactive $^{153}SmCl_3$@MWCNTs with the total mixture containing roughly 100 MBq. The sample was dispersed by sonication for 5 min and the procedure of functionalization was followed as described above for the cold materials. After deprotection, the obtained material was re-precipitated in EtOH, filtered, washed with 0.1 M HCl solution and water. Radioactivity of aliquots sampled before and after the functionalization was measured using γ-counting (LKB Wallac 1282 Compugamma, PerkinElmer). The % recovery was measured as 49.2%, indicating half of the radioactivity was lost during the different processing and centrifugation steps. The presence of the free ^{153}Sm in the samples was examined by thin layer chromatography (TLC) followed by γ-counting. No free ^{153}Sm was present in the solvent front, indicating all radioactive ^{153}Sm remained sealed in the cavity of the functionalized MWCNTs. The functionalized $^{153}SmCl_3$@MWCNTs, referred to as $^{153}SmCl_3$@MWCNTs-NH_2, were directly used for biodistribution studies.

Characterization of functionalized $SmCl_3$@MWCNTs-NH_2

Kaiser test. It was performed to determine the concentration of amine groups on the functionalized $SmCl_3$@MWCNTs-NH_2. In a typical test, 0.3–0.5 mg of $SmCl_3$@MWCNTs-NH_2 were dispersed in a mixture of phenol (75 μL, 80% in ethanol) and KCN (100 μL in H_2O/pyridine) solution and sonicated for 2 min in an ultrasonic bath. Subsequently, 75 μL of ninhydrin solution (6% in ethanol) were added, and the mixture was heated at 120 °C for 10 min. Then, it was cooled and diluted with 60% ethanol in water to a final volume of 3 mL. After centrifugation (3000 rpm, 10 min), the absorption spectrum of the supernatant was measured, using as blank a solution obtained in the same way but without MWCNTs. The absorbance maximum at 570 nm was used to calculate the amine loading in the $SmCl_3$@MWCNTs-NH_2 samples (ε = 15 000 M^{-1} cm^{-1}). Reported values are an average of two separate measurements. UV-vis spectra were recorded on a Cary 5000 spectrophotometer (Varian) using 1 cm path quartz cuvettes main paragraph text follows directly on here.

Thermogravimetric analysis (TGA). Pristine, filled and functionalized MWCNTs samples were measured using Q500 (TA Instruments) to record TGA under N_2 or air, by equilibrating at

100 °C, and following a ramp of 10 °C min^{-1} up to 800 °C with a flow rate of 90 mL min^{-1}. About 0.7 mg of sample per each analysis was required. Reported graphs are representative of at least two separate measurements. Empty carbon nanotubes were analyzed also using a TA Q-5000-IR TGA instrument, with a heating rate of 10 °C min^{-1} up to 900 °C under an air gas flow of 25 mL min^{-1}.

Electron microscopy. For electron microscopy studies, MWCNTs samples were dispersed in ethanol by sonication and the dispersions were drop-casted onto lacey carbon-coated copper grids (300 mesh, from TedPella). High resolution transmission electron microscopy (HRTEM) and high angle annular dark field scanning transmission electron microscopy (HAADF STEM) images were acquired on a FEI Tecnai G2 F20 HRTEM at 200 kV, which is coupled to an EDAX super ultra-thin window (SUTW) X-ray detection system for energy dispersive X-ray (EDX) composition studies.

Cell toxicity assays

B16F10-Luc melanoma cells and J774 macrophage cells were cultured in Advanced RPMI-1640 media supplemented with 10% FBS, 100 IU mL^{-1}, penicillin, and 100 μg mL^{-1} streptomycin at 37 °C in 5% CO_2 atmosphere.

Cells were seeded at a density of 8000 cells per well in flat-bottomed 96-well plates and left to adhere overnight. The $^{152}SmCl_3$@MWCNTs and $^{152}SmCl_3$@MWCNTs-NH_2 were dispersed in 1% Pluronic F-127 in saline (0.9% NaCl) at 1 mg mL^{-1}. The functionalized material was also dispersed in water without the presence of the surfactant. Cells were then treated with MWCNTs dispersions diluted in complete media at final concentrations of 10, 50, 100 μg mL^{-1} for 72 h. Cells incubated with complete media containing 10% DMSO were used as a positive control. To avoid risk of interference from the intrinsic absorbance of CNTs at 490 nm, the modified version of the LDH protocol was used to assess the cytotoxicity.[20] Eqn (1) was used to calculate the cells survival with modified LDH assay:

$$\%\ \text{Cell survival} = \frac{\text{A 490 nm of treated cells}}{\text{A 490 nm of untreated cells}} \times 100 \qquad (1)$$

Biodistribution study of $^{153}SmCl_3$@MWCNTs-NH_2 in naïve mice by γ-counting

All *in vivo* experiments were conducted under the authority of project and personal licenses granted by the UK Home Office and the UKCCCR Guidelines (1998). Female C57BL/6 mice aged 6–8 weeks were purchased from Envigo (UK) and used for all *in vivo* studies.

Tissue biodistribution studies of $^{153}SmCl_3$@MWCNTs-NH_2 including assessments of blood circulation and excretion profiles in mice were performed. The radioactive $^{153}SmCl_3$@MWCNTs-NH_2 were re-suspended in 1% Pluronic F-127 saline solution for injection to mice. The final concentration was approx. 1 mg mL^{-1}, containing ~1.5 MBq per 200 μL. Mice were given 200 μg of $^{153}SmCl_3$@MWCNTs-NH_2 intravenously, *via* a tail vein. To obtain the excretion profile, mice were housed singly in metabolic cages in which animals had free access to water but not food. After 24 h, urine and feces were collected from individual cages and measured by γ-counting. For blood profiles, blood samples were collected in heparinized capillaries from 4 min up to 24 h after injection and measured by γ-counting. At 1, 4, and 24 h after collecting the blood, the animals (n = 3) were perfused with 25 mL of heparinized saline (50 IU mL^{-1}) *via* the left ventricle of the heart to clear $^{153}SmCl_3$@MWCNTs-NH_2 remaining in blood. Major organs including skin, liver, spleen, heart, lung, muscle, bone, brain, stomach and intestine were excised and weighed, and the radioactivity was measured by γ-counting. The percentages of injected doses per organ (% ID per organ) and per gram of tissue (% ID g^{-1} of organ) were calculated for each organ.

Biodistribution study of $^{153}SmCl_3$@MWCNTs-NH_2 in tumor-bearing mice by γ-counting

Organ biodistribution profiles of $^{153}SmCl_3$@MWCNTs-NH_2 were determined in three types of *in vivo* tumors, all implanted in C57BL/6 mice. To establish subcutaneous (s.c.) B16F10-tumor model, mice were inoculated with B16F10-Luc cells (106 cells in 0.1 mL of PBS) at both flanks. Experimental lung metastatic model was established by intravenous injection of B16F10-Luc cells (5×10^5 cells in 0.2 mL of PBS). Intracranial GL261 glioma model was established by stereotactically-guided injection of 1.25×10^5 GL261-Luc glioma cells (3 μL) into the right hemisphere using a Hamilton syringe (Harvard Apparatus, UK) with a 26-gauge needle at 0.2 μL min^{-1}.[25] Tumor growth monitoring was carried out by caliber measurement (for s.c. tumors) or bioluminescence imaging (for lung metastases and glioma tumors) using an IVIS Lumina III system (PerkinElmer, UK).

When tumors reached ~8 mm in diameter (for s.c. tumors) or at 1–2 weeks post inoculation (for lung metastases and glioma tumors), mice were intravenously injected with $^{153}SmCl_3$@MWCNTs-NH_2 at a dose of 200 μg CNTs in 200 μL 1% Pluronic F-127 saline containing (~1.5 MBq). Organ (including tumors) biodistribution and blood circulation profiles were examined at 1 and 24 h post as described for naïve mice.

Conclusions

This work reports a rapid method for exohedral functionalization of MWCNTs designed for radioactivity delivery. The optimized aryl diazonium chemistry can be carried out in one hour, offering an adequate level of functionalization sufficient to improve the water-dispersibility of MWCNTs and a platform to introduce subsequent biomolecules. Covalent attachment of triazine derivative though sp^2 carbon network modification resulted in no leakage of the encapsulated material, indicating that the inner part of tubes remained intact. In mice, organ biodistribution of the aryl functionalized radioactive MWCNTs showed high accumulation in lung followed by liver and spleen, suggesting the suitability to passively target these tumor types in future efficacy studies in animals.

Author contributions

AG: investigation, visualization, methodology, validation, writing – original draft. JT-WW: investigation, formal analysis, visualization, validation, writing – original draft. RK: investigation, formal analysis, visualization. MM: investigation, visualization. EP: investigation, visualization. RF: investigation. J-CS: resources, supervision. GT: resources, supervision, funding acquisition, writing – review & editing. BB: resources, supervision, funding acquisition, writing – review & editing. KTA-J: conceptualization, resources, supervision, validation, visualization, funding acquisition, writing – review & editing. TDR: conceptualization, resources, supervision, validation, visualization, funding acquisition, writing – review & editing.

Conflicts of interest

There are no conflicts to declare.

Acknowledgements

We thank Thomas Swan & Co. Ltd for supplying the Eli-carb® MWCNTs. This work was supported by European Union's Seventh Framework Programme FP7, Project ''RADDEL'' [grant number 290023], Worldwide Cancer Research [grant number 12-1054], Biotechnology and Biological Sciences Research Council [grant number BB/J008656/1], European Union HORIZON 2020 MSCA RISE 2016, Project Carbo-Immap [grant number 734381], ''Severo Ochoa'' Programme for Centres of Excellence in R&D [grant numbers SEV-2015-0496, SEV-2017-0706], and Generalitat de Catalunya 2017 [grant number SGR 327].

References

1 (*a*) S. Iijima, *Nature*, 1991, **354**, 56; (*b*) L. Ortolani, F. Houdellier, M. Monthioux and V. Morandi, *Carbon*, 2010, **48**, 3050.

2 (*a*) C. Ménard-Moyon, E. Venturelli, C. Fabbro, C. Samorì, T. Da Ros, K. Kostarelos, M. Prato and A. Bianco, *Expert Opin. Drug Discovery*, 2010, **5**, 691; (*b*) C. Fabbro, A. Ali-Boucetta, T. Da Ros, K. Kostarelos, A. Bianco and M. Prato, *Chem. Commun.*, 2012, **48**, 3911; (*c*) A. Battigelli, C. Ménard-Moyon, T. Da Ros, M. Prato and A. Bianco, *Adv. Drug Delivery Rev.*, 2013, **65**, 1899.

3 R. Klingeler and R. B. Sim, *Carbon nanotubes for biomedical applications*, Springer, Berlin, Heidelberg, 2011.

4 (*a*) A. Vyalikh, A. U. B. Wolter, S. Hampel, D. Haase, M. Ritschel, A. Leonhardt, H.-J. Grafe, A. Taylor, K. Krämer, B. Büchner and R. Klingeler, *Nanomedicine*, 2008, **3**, 321; (*b*) M. del Carmen Giménez-López, F. Moro, A. La Torre, C. J. Gómez-García, P. D. Brown, J. van Slageren and A. N. Khlobystov, *Nat. Commun.*, 2011, **2**, 407; (*c*) M. Martincic and G. Tobias, *Expert Opin. Drug Delivery*, 2015, **12**, 563.

5 (*a*) S. Westrøm, M. Malenge, I. S. Jorstad, E. Napoli, Ø. S. Bruland, T. B. Bønsdorff and R. H. Larsen, *J. Labelled Compd. Radiopharm.*, 2018, **61**, 472; (*b*) M. V. Zyuzin, D. Antuganov, Y. V. Tarakanchikova, T. E. Karpov, T. V. Mashel, E. N. Gerasimova, O. O. Peltek, N. Alexandre, S. Bruyere, Y. A. Kondratenko, A. R. Muslimov and A. S. Timin, *ACS Appl. Mater. Interfaces*, 2020, **12**, 31137.

6 S. Y. Hong, G. Tobias, K. T. Al-Jamal, B. Ballesteros, H. Ali-Boucetta, S. Lozano-Perez, P. D. Nellist, R. B. Sim, C. Finucane, S. J. Mather, M. L. H. Green, K. Kostarelos and B. G. Davis, *Nat. Mater.*, 2010, **9**, 485.

7 S. De Munari, S. Sandoval, E. Pach, B. Ballesteros, G. Tobias, D. C. Anthony and B. G. Davis, *Inorg. Chim. Acta*, 2019, **495**, 118933.

8 (*a*) R. Singh, D. Pantarotto, L. Lacerda, G. Pastorin, C. Klumpp, M. Prato, A. Bianco and K. Kostarelos, *Proc. Natl. Acad. Sci. U. S. A.*, 2006, **103**, 3357; (*b*) M. R. McDevitt, D. Chattopadhyay, J. S. Jaggi, R. D. Finn, P. B. Zanzonico, C. Villa, D. Rey, J. Mendenhall, C. A. Batt, J. T. Njardarson and D. A. Scheinberg, *PLoS One*, 2007, **2**, e907; (*c*) X. Deng, S. Yang, H. Nie, H. Wang and Y. Liu, *Nanotechnology*, 2008, **19**, 075101; (*d*) Z. Liu, W. Cai, L. He, N. Nakayama, K. Chen, X. Sun, X. Chen and H. Dai, *Nat. Nanotechnol.*, 2007, **2**, 47; (*e*) A. Ruggiero, C. H. Villa, J. P. Holland, S. R. Sprinkle, C. May, J. S. Lewis, D. A. Scheinberg and M. R. McDevitt, *Int. J. Nanomed.*, 2010, **5**, 783; (*f*) M. Das, S. R. Datir, R. P. Singh and S. Jain, *Mol. Pharmaceutics*, 2013, **10**, 2543; (*g*) J. T.-W. Wang, L. Cabana, M. Bourgognon, H. Kafa, A. Protti, K. Venner, A. M. Shah, J. K. Sosabowski, S. J. Mather, A. Roig, X. Ke, G. Van Tendeloo, R. T. M. de Rosales, G. Tobias and K. T. Al-Jamal, *Adv. Funct. Mater.*, 2014, **24**, 1880; (*h*) J. T.-W. Wang, C. Fabbro, E. Venturelli, C. Ménard-Moyon, O. Chaloin, T. Da Ros, L. Methven, A. Nunes, J. K. Sosabowski, S. J. Mather, M. K. Robinson, J. Amadou, M. Prato, A. Bianco, K. Kostarelos and K. T. Al-Jamal, *Biomaterials*, 2014, **35**, 9517; (*i*) T. Peci, T. J. S. Dennis and M. Baxendale, *Carbon*, 2015, **87**, 226.

9 H. Ge, P. J. Riss, V. Mirabello, D. G. Calatayud, S. E. Flower, R. L. Arrowsmith, T. D. Fryer, Y. Hong, S. Sawiak, R. M. J. Jacobs, S. W. Botchway, R. M. Tyrrell, T. D. James, J. S. Fossey, J. R. Dilworth, F. I. Aigbirhio and S. I. Pascu, *Chem*, 2017, **3**, 437.

10 C. Spinato, A. P. Ruiz de Garibay, M. Kierkowicz, E. Pach, M. Martincic, R. Klippstein, M. Bourgognon, J. T.-W. Wang, C. Menard-Moyon, K. T. Al-Jamal, B. Ballesteros, G. Tobias and A. Bianco, *Nanoscale*, 2016, **8**, 12626.

11 (*a*) D. Pantarotto, R. Singh, D. McCarthy, M. Erhardt, J.-P. Briand, M. Prato, K. Kostarelos and A. Bianco, *Angew. Chem., Int. Ed.*, 2004, **43**, 5242; (*b*) Z. Markovic, B. Todorovic-Markovica, D. Kleut, N. Nikolic, S. Vranjes-Djuric, M. Misirkic, L. Vucicevic, K. Janjetovic, L. Harhaji, B. Babic-Stojic, M. Dramicanin and V. Trajkovic, *Biomaterials*, 2007, **28**, 5437.

12 J. M. González-Domínguez, A. Santidrián, A. Criado, C. Hadad, M. Kalbáč and T. Da Ros, *Chem. – Eur. J.*, 2015, **21**, 18631.

13 J. T.-W. Wang, R. Klippstein, M. Martincic, E. Pach, R. Feldmann, M. Sefl, Y. Michel, D. Asker, J. Sosabowski, M. Kalbáč, T. Da Ros, C. Menard-Moyon, A. Bianco, I. Kyriakou, D. Emfietzoglou, J.-C. Saccavini, B. Ballesteros, K. T. Al-Jamal and G. Tobias, *ACS Nano*, 2020, **14**, 129.

14 B. Ballesteros, G. Tobias, M. A. H. Ward and M. L. H. Green, *J. Phys. Chem. C*, 2009, **113**, 2653.
15 M. Martincic, E. Pach, B. Ballesteros and G. Tobias, *Phys. Chem. Chem. Phys.*, 2015, **17**, 31662.
16 M. Martincic, S. Vranic, E. Pach, S. Sandoval, B. Ballesteros, K. Kostarelos and G. Tobias, *Carbon*, 2019, **141**, 782.
17 (*a*) J. L. Bahr and J. M. Tour, *Chem. Mater.*, 2001, **13**, 3823; (*b*) J. L. Bahr, J. Yang, D. V. Kosynkin, M. J. Bronikowski, R. E. Smalley and J. M. Tour, *J. Am. Chem. Soc.*, 2001, **123**, 6536; (*c*) B. K. Price and J. M. Tour, *J. Am. Chem. Soc.*, 2006, **128**, 12899.
18 (*a*) J. Mateos-Gil, L. Rodríguez-Pérez, M. Moreno Oliva, G. Katsukis, C. Romero-Nieto, M. Á. Herranz, D. M. Guldi and N. Martín, *Nanoscale*, 2015, **7**, 1193; (*b*) C. Ménard-Moyon, C. Fabbro, M. Prato and A. Bianco, *Chem. – Eur. J.*, 2011, **17**, 3222.
19 G. Schmidt, S. Gallon, S. Esnouf, J.-P. Bourgoin and P. Chenevier, *Chem. – Eur. J.*, 2009, **15**, 2101.
20 H. Ali-Boucetta, K. T. Al-Jamal, K. H. Müller, S. Li, A. E. Porter, A. Eddaoudi, M. Prato, A. Bianco and K. Kostarelos, *Small*, 2011, **7**, 3230.
21 R. D. Gately and M. Panhuis, *Beilstein J. Nanotechnol.*, 2015, **6**, 508.
22 J. T.-W. Wang, C. Spinato, R. Klippstein, P. M. Costa, M. Martincic, E. Pach, A. P. Ruiz De Garibay, C. Menard-Moyon, R. Feldman, Y. Michel, M. Åefl, I. Kyriakou, D. Emfietzoglou, J.-C. Saccavini, B. Ballesteros, G. Tobias, A. Bianco and K. T. Al-Jamal, *Carbon*, 2020, **162**, 410.
23 V. Georgakilas, K. Kordatos, M. Prato, D. M. Guldi, M. Holzinger and A. Hirsch, *J. Am. Chem. Soc.*, 2002, **124**, 760.
24 P. M. Costa, M. Bourgognon, J. T.-W. Wang and K. T. Al-Jamal, *J. Controlled Release*, 2016, **241**, 200.
25 H. Kafa, J. T.-W. Wang, N. Rubio, R. Klippstein, P. M. Costa, H. A. Hassan, J. K. Sosabowski, S. S. Bansal, J. E. Preston, N. J. Abbott and K. T. Al-Jamal, *J. Controlled Release*, 2016, **225**, 217.
26 (*a*) H. Kafa, J. T.-W. Wang, N. Rubio, K. Venner, G. Anderson, E. Pach, B. Ballesteros, J. E. Preston, N. J. Abbott and K. T. Al-Jamal, *Biomaterials*, 2015, **53**, 437; (*b*) J. T.-W. Wang, N. Rubio, H. Kafa, E. Venturelli, C. Fabbro, C. Ménard-Moyon, T. Da Ros, J. K. Sosabowski, A. D. Lawson, M. K. Robinson, M. Prato, A. Bianco, F. Festy, J. E. Preston, K. Kostarelos and K. T. Al-Jamal, *J. Controlled Release*, 2016, **224**, 22.
27 M. Kierkowicz, E. Pach, A. Santidrián, S. Sandoval, G. Gonçalves, E. Tobías-Rossell, M. Kalbáč, B. Ballesteros and G. Tobias, *Carbon*, 2018, **139**, 922.
28 M. Martincic, C. Frontera, E. Pach, B. Ballesteros and G. Tobias, *Polyhedron*, 2016, 116.

